CrossMark

A promising porous polymer-nanoclay hydrogel nanocomposite as water reservoir material: synthesis and kinetic study

Ali Olad[1] · Hamid Zebhi[1] · Dariush Salari[1] · Abdolreza Mirmohseni[1] ·
Adel Reyhanitabar[2]

Abstract A porous hydrogel nanocopmposite based on biodegradable salep and montmorillonite (MMT) was synthesized by in-situ free radical graft polymerization of salep chains with acrylic acid (AA) monomers. The chemical structure and morphological properties of the prepared hydrogels was evaluated by FTIR spectroscopy, X-ray diffraction and SEM techniques. The effect of reaction variables such as crosslinker, initiator, monomer and clay contents on equilibrium water absorption capacity and swelling kinetic of hydrogel were investigated and optimized. Swelling behavior of the hydrogels in various pH and saline solutions was also studied. Incorporation of MMT into hydrogel matrix caused the formation of porous hydrogel network. These porous structures resulted in higher water uptake capacity and swelling rate in hydrogel nanocomposite in comparison to neat hydrogel sample. Moreover, hydrogel nanocomposite sample exhibited proper salt and pH-sensitive behavior. High swelling capacity and rate, porosity, salt and pH sensitivity make hydrogel nanocomposite a profitable candidate in agricultural and horticultural applications, such as water reservoir system.

Keywords Hydrogel nanocomposite · Salep · Montmorillonite · Water reservoir · Swelling kinetic

✉ Ali Olad
  a.olad@yahoo.com

[1] Polymer Composite Research Laboratory, Department of Applied Chemistry, Faculty of Chemistry, University of Tabriz, Tabriz, Iran

[2] Department of Soil Science, Faculty of Agriculture, University of Tabriz, Tabriz, Iran

1 Introduction

Water absorbent hydrogels are kind of cross-linked polymers that can absorb water 100 times more than their dry weight. These polymers not only can absorb large amount of water, but also have high water retention potential [1–3]. A suitable water absorbent hydrogel must have properties such as hydrophilicity, high swelling ratio in contact with water based solutions, because of void spaces made due to existence of charge repulsion in cross-linked structure [4–6]. To achieve above as mentioned structure, a common method is graft polymerization of monomers onto natural polysaccharides, especially vinylic monomers.

Graft polymerization of acrylic acid (AA) monomer has attracted much attention in recent years because of its high potential to be commercially produced. AA graft copolymers are used in some industries such as drug delivery, coagulation process in water treatment, precipitation of aqueous suspensions, resins fabrication, baby diapers, and agricultural applications. In all of these applications, high water uptake and better water retention are the most important factors [7, 8].

Some properties of natural polymers make them more profitable choices as water absorbent hydrogels over synthetic polymers. The use of natural polymers, including alginate, chitosan, and starch besides being biodegradable and biocompatible, end in reduction of petrochemical based monomers demand. Salep is a multi-component polysaccharide that can be obtained from orchid route. This plant's origin is some Middle East countries such as Iran, Turkey, and India and it is mostly used as concentrating agent in ice cream and fruit juices [9–11]. In several scientific researches, salep polysaccharide has been used as biodegradable part of the polymeric hydrogels [12, 13].

In addition, high production cost and low mechanical strength of hydrogels, especially in natural based ones, are the main defects and so they limit natural-based hydrogels to be commercialized. Mica, kaolin, alumina, and clays [such as montmorillonite (MMT)] have been lastly used to improve mechanical properties and cause cost affectivity of hydrogels [14–18].

To the best of our knowledge, synthesis of the salep-g-acrylic acid/MMT (Hyd/MMT) hydrogel nanocomposite has not been reported elsewhere. Therefore, herein we report the synthesis of a novel porous hydrogel nanocomposite based on the salep, AA, and MMT. The effect of clay content on the swelling capacity and water absorption rate of the Hyd/MMT was investigated. The water absorption capacity of the Hyd/MMT in different saline and pH solutions was measured. Also, swelling kinetic and water transport mechanism of hydrogel samples were evaluated in distilled water as swelling medium.

2 Experimentals

2.1 Materials

AA, N,N′-methylene bisacrylamide (MBA), ammonium persulfate (APS), and sodium hydroxide were purchased from Merck. Ethanol (96%) was purchased from Mojallali reagent chemicals Co. (Iran, Tabriz). Palmate-tuber salep was purchased from a supplier in Tabriz, Iran. All solutions were prepared with doubly distilled water.

2.2 Characterization methods

The FTIR spectra of Salep, MMT, Hyd, and Hyd/MMT were recorded by a Bruker Tensor 27 FTIR at the wavenumber range of 400–4000 cm^{-1} using samples prepare as KBr pellets. Wide angle X-ray diffraction patterns of Hyd, MMT, and Hyd/MMT were also measured using a Siemens D500 X-ray diffractometer (Siemens AG, Karlsruhe, Germany) with Cu Kα radiation in 2Θ range of 2°–70°. The surface morphologies of Salep, Hyd, and Hyd/MMT were studied using MIRA3 FEG-SEM (Tescan, Czech) scanning electron microscope (SEM).

2.3 Synthesis of Hyd/MMT nanocomposite hydrogel

At first, 0.3 g of salep powder was mixed adequately with 30 mL distilled water in a three necked round-bottomed flask equipped with a mechanical stirrer, a reflux condenser, and a nitrogen purge line. This blend stirred continuously with the rate of 600 rpm at 60 °C to obtain a homogenous viscous solution. Then, certain amount of MMT (0–30 wt% with respect to salep) was sonicated with

ultrasonic probe for 30 min in distilled water and added to the prepared solution while stirring. After purging with nitrogen to remove the dissolved oxygen, certain amount of 65% neutralized AA monomers (0.1–0.4 mol/L) and proper amount of MBA (0.01–0.04 mol/L) as crosslinker were added into the mixture. At the next step, certain amount of APS (0.015–0.037 mol/L) were added to the solution as an initiator. Thereafter, temperature of the reaction mixture was raised up to 70 °C and maintained in this condition for 4 h to complete the polymerization process. The obtained gel like product cut to small pieces, and then it was immersed in ethanol for 24 to remove unreacted species. Then, white colored dehydrated gel was dried in an oven at 70 °C for 24 h.

2.4 Investigation of swelling behavior of prepared samples

To study the swelling behavior of the synthesized samples, 0.05 g of dried hydrogel sample was transferred into an empty tea bag and then it was immersed in 400 mL distilled water for 24 h at room temperature. Then, the swollen hydrogel was taken out of the distilled water in certain time intervals and was weighted after removing the surface water by a filter paper. The equilibrium swelling ratio [S_{eq} (g/g)] was calculated using the following equation:

$$S_{eq}(g/g) = \frac{W_s - W_d}{W_d} \quad (1)$$

where W_s (g) is the weight of the swollen hydrogel sample, and W_d (g) is the weight of the dry hydrogel sample.

2.4.1 Swelling kinetic studies

To study the swelling kinetic of hydrogels, the Schott second ordered kinetic formula was used [19].

$$\frac{t}{W} = A + Bt \quad (2)$$

$$B = \frac{1}{W_\infty} \quad (3)$$

$$A = \frac{1}{\left(\frac{dW}{dt}\right)_0} \quad (4)$$

$$k_s = \frac{1}{AW_\infty^2} \quad (5)$$

In which W and W_∞ are absorbed water amount at t time and equilibrium time, respectively. B is inverse maximum swelling, A is inverse initial swelling rate and k_s is swelling

rate constant. After plotting the t/W versus t trend, A and B can be obtained from intercept and slope, respectively.

2.4.2 Water absorption mechanism and diffusion coefficient

To investigate the water diffusion mechanism in hydrogels, following formula was used which was valid for initial 60% of water absorption process [20, 21].

$$\frac{W_t}{W_\infty} = kt^n \tag{6}$$

In this formula, W_t and W_∞ show absorbed amount of water in t and equilibrium time respectively and k is specific relative constant and n is a factor which shows the diffusion mechanism. For Fickian diffusion mechanism, n is 0.45–0.5 and for non-Fickian diffusion n is 0.5–1. For case-II diffusion or controlled transmission n is 1 and for supercase-II diffusion n is more than 1. By drawing the ln (W_t/W_∞) on ln (t), swelling ability (n) and swelling constant (k) are obtained from the slope and intercept of trend, respectively.

Other factor that is investigated in hydrogels swelling manner is diffusion coefficient. For this aim, short time approximation method is used. This method is valid only for initial 60% of swelling. Spherical hydrogel samples diffusion coefficient is obtained from the following equation [20, 21]:

$$\frac{W_t}{W_\infty} = 4\left(\frac{Dt}{\pi r^2}\right)^{\frac{1}{2}} \tag{7}$$

In this equation, D (cm^2/min) is diffusion coefficient, t (min) is time and r (cm) is the spherical hydrogels radius. By drawing the W_t/W_∞ versus $t^{1/2}$, diffusion coefficient is obtained from the line slope (below formula) [20, 21]:

$$k = 4\left(\frac{D}{\pi r^2}\right)^{\frac{1}{2}} \tag{8}$$

2.4.3 Water absorption rate study

Other important diffusion parameter is water absorption rate constant. According to the water absorption equation, W_t and W_∞ are water absorption in time t and equilibrium water absorption respectively. t is time factor in minute and k_w is water absorption rate constant [22].

$$W_t = W_\infty\left(1 - e^{-k_w t}\right) \tag{9}$$

By using Eq. (9), and plotting the $-\ln\left(1 - W_t/W_\infty\right)$ versus t, the water absorption rate constant is obtained from the line slope.

2.5 Investigation of pH sensitivity of prepared hydrogels

To investigate the pH sensitivity of hydrogels, acidic and basic solutions with different pH range of 2–12 were prepared by using 0.1 M solutions of NaOH and HCl. Then, 0.05 g of dried hydrogel sample was immersed in solutions with different pH values. Thereafter, the equilibrium swelling ratio determined similar to the method described in Sect. 2.4.

2.6 Effect of salt solutions on swelling

The procedures for these experiments were the same as described in Sect. 2.4, except that different salt solutions were used (NaCl, $CaCl_2$, and $FeCl_3$) instead of distilled water. Additionally, the swelling behavior of the samples in solutions with various concentrations of NaCl was measured.
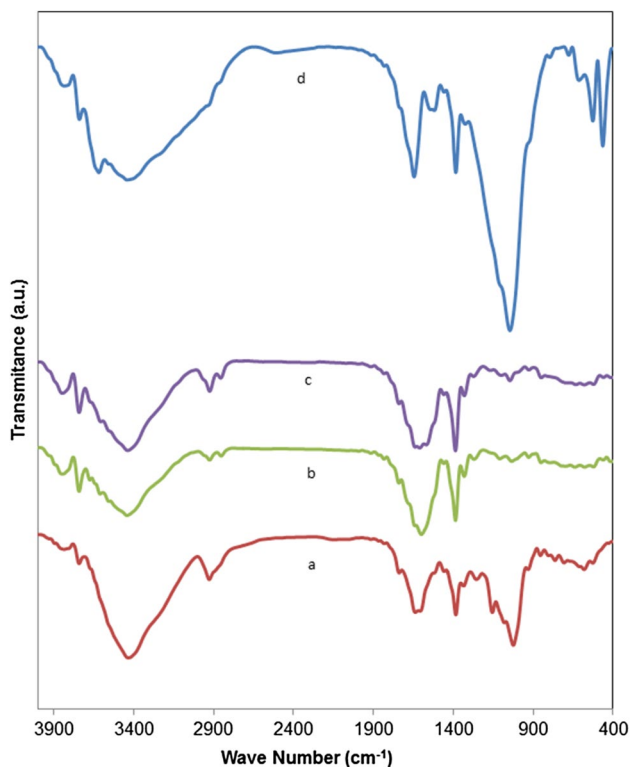
3 Results and discussion

3.1 Synthesis and characterization

Figure 1 illustrates the proposed mechanism for the crosslinking and graft polymerization process of AA onto salep chains. The hydrogel sample was synthesized by free radical graft polymerization of AA monomers with salep chains. This process was carried out in an aqueous medium using APS as a radical initiator and MBA as a crosslinking agent. Decomposition of APS initiator under heating at 60 °C and N_2 atmosphere generates sulfate anion-radicals. These free radicals abstract hydrogen atom from the hydroxyl functional groups of the salep chains, leading to formation of macro radicals. Later, radically activated AA monomers can be grafted onto these active macro radicals. In this step, MBA cross-linked the macro radicals and AA monomers and so a 3D network was formed. During network formation, MMT nanolayers were trapped in the network structure and acted as reinforcing agent.

The grafting and MMT incorporation into hydrogel network was confirmed by comparing the FTIR spectra of salep, Hyd, MMT, and Hyd/MMT nanocomposite. As shown in Fig. 2a, for FT-IR spectrum of MMT, the sharp peak at 1045 cm^{-1} is due to Si–O stretching vibration and bands in 3441 and 3619 cm^{-1} are due to O–H and N–H stretching vibration, respectively. Also, the absorption band in 1645 cm^{-1} implies to flexural vibration of H–O–H and existing peaks in 526 and 464 cm^{-1} are representing Al–O and Mg–O stretching vibrations [23, 24]. Main polysaccharide parts of salep absorbing bands are shown in Fig. 2b. A wide peak in 3441 cm^{-1} is due to
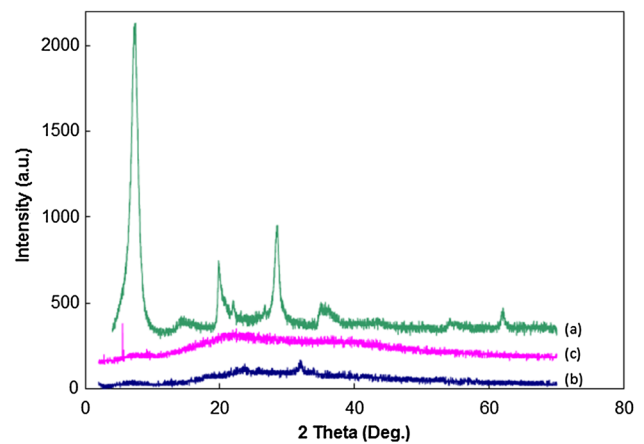
Fig. 1 Outline of the synthesis mechanism of Hyd/MMT hydrogel nanocomposite

Fig. 2 FT-IR Spectra of MMT (*a*), Salep (*b*), Hyd (*c*), and Hyd/MMT (*d*)

Fig. 3 X-ray diffraction (XRD) patterns of the MMT (*a*), Hyd (*b*), and Hyd/MMT (*c*)

stretching vibration of O–H groups in polysaccharide structure. A peak in 1638 cm^{-1} implies to stretching vibration of C=O group in glucomannan structure. Existing bands in 900–1200 cm^{-1} zone are according to stretching vibration of C–O–C ether groups and C–OH alcoholic groups in glucomannan. According to FT-IR spectrum of hydrogel (Fig. 2c), absorbing peak in 3443 cm^{-1} is due to stretching vibration of OH group of carboxylic acid group in hydrogel structure and also a peak in 1599 cm^{-1} implies to stretching vibration of carbonyl (C=O) group [19]. By comparing the FT-IR spectrum of salep and hydrogel, it is obtained that stretching vibration peak of carbonyl group is shifted from 1638 to 1599 cm^{-1} which is because of grafting salep with AA. In Hyd/MMT nanocomposite hydrogel FTIR spectrum (Fig. 2d), in addition to the above mentioned peaks in neat hydrogel spectrum, strong absorbing band at 1024 cm^{-1} relating to Si–O groups of MMT structure, confirms the MMT incorporation into hydrogel network. Also it should be mentioned that this peak has a small shift from 1045 to 1024 cm^{-1}.

Figure 3 shows the XRD pattern of MMT, Hyd, and Hyd/MMT nanocomposite hydrogel. As shown in Fig. 3a, the existing peak in 2Θ = 7.48˚ is related to pure MMT, referring to the basal plane and corresponding to the interlamelar distance (at the direction of 001).

XRD pattern of Hyd (Fig. 3b) also shows weak peaks in 2Θ = 24˚ and 2Θ = 33˚ which are related to the amorphous structure of hydrogel. As shown in Fig. 3c, in XRD pattern of Hyd/MMT nanocomposite, characteristic peak of MMT (2Θ = 7.48˚) was shifted to lower degrees (2Θ = 5.54˚) and severely decreased which confirms the increase in MMT layers distances at the direction of (001). It should be noted that, this increase in MMT layers distance is result of polymer chains entrance between the empty spaces of MMT layers [25]. Furthermore, disappearing other peaks of MMt in Hyd/MMT XRD pattern proves the clay layers separation as a result of silicate layers exfoliation. Well dispersed clay in polymeric matrix was an essential factor to obtain a highly exfoliated nanocomposite. In exfoliated nanocomposite most of layers of clay are available, so the interaction between materials is in its maximum state and this is confirmed by studying the XRD pattern of nanocomposite.

In order to study the surface morphology of the salep, Hyd, and Hyd/MMT hydrogel nanocomposite, SEM technique was used. Figure 4 shows SEM images of salep (a, b), Hyd (b, c) and Hyd/MMT nanocomposite hydrogel (d, e) with two different magnifications. As it is shown in Fig. 4a–d, surface structure of salep and prepared Hyd is homogenous and does not show any porous structure. But, by comparing the SEM images of Hyd/MMT nanocomposite hydrogel with neat hydrogel, it is obtained that the structure of Hyd/MMT nanocomposite hydrogel is highly porous. Therefore, it can be expected that Hyd/MMT sample will have high swelling ratio compared to the neat hydrogel. This expectancy was confirmed with swelling experimental data which is given in Sect. 3.5.
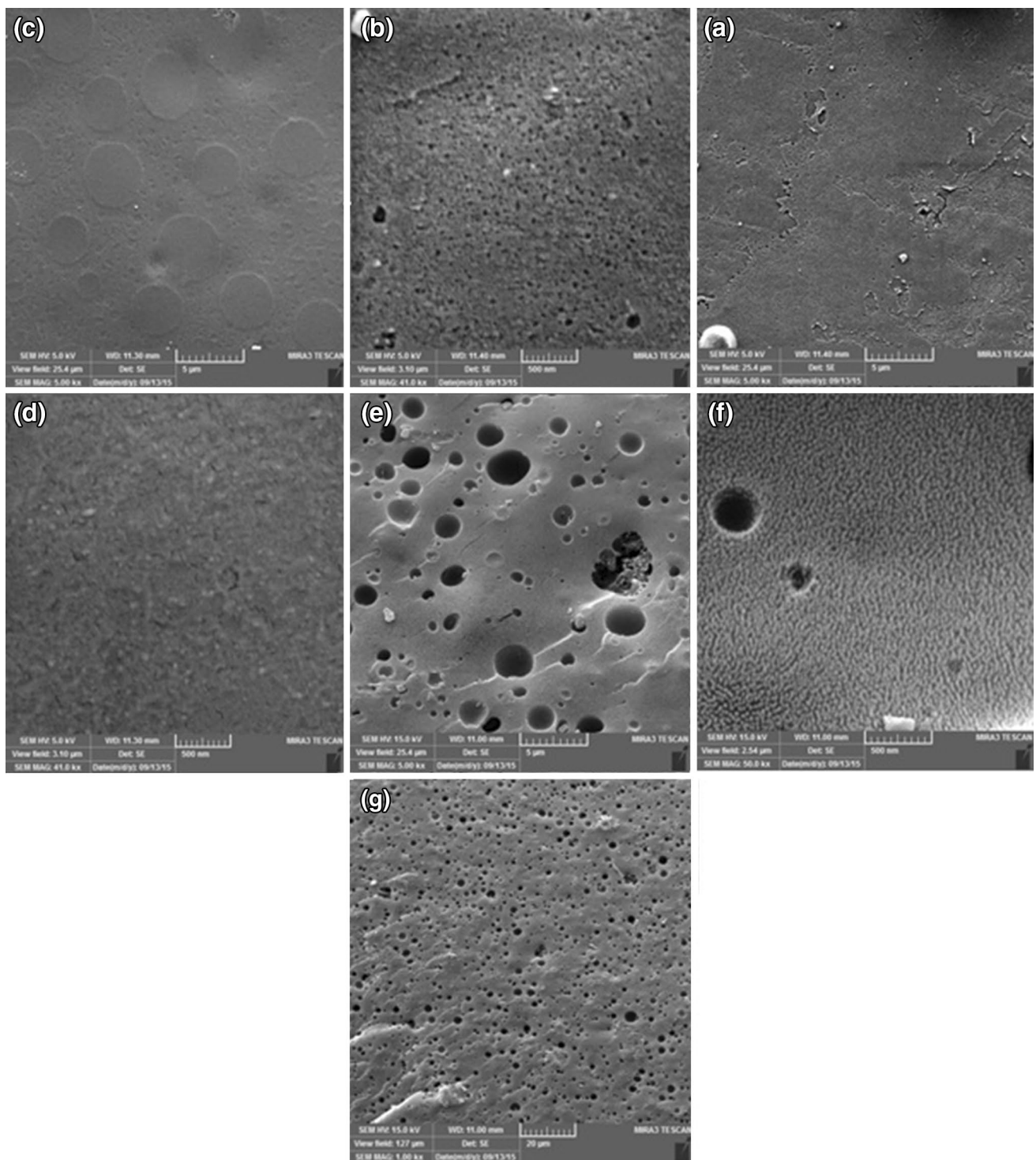
Fig. 4 SEM micrographs for Salep (**a**, **b**), Hyd (**c**, **d**), and Hyd/MMT (**e**, **f**, **g**)

3.2 Effect of MBA crosslinker concentration on swelling behavior

Cross linking agent is an essential component that its concentration affects cross linking density as well as water absorption ability of hydrogel which is defined by Flory's network theory [26]. Figure 5a represents the equilibrium water absorption capacity of the prepared superabsorbent hydrogels at different MBA concentration. As shown in Fig. 5a, the highest swelling ratio (258 g/g) was obtained

Fig. 5 Dependence of equilibrium water absorption capacity as a function of crosslinker (MBA) (**a**), monomer (AA) (**b**), initiator (APS) (**c**), and %MMT (**d**)
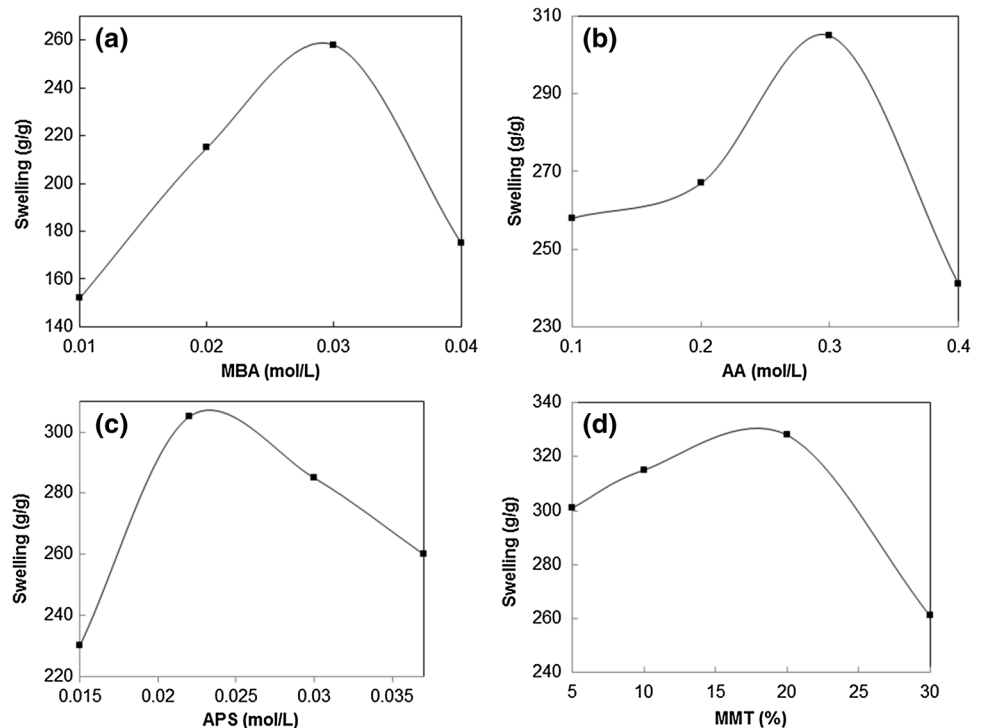
at 0.03 mol/L of MBA. At MBA concentrations lower than 0.03 mol/L, swelling ratio is decreased which is because of the existence of soluble materials in hydrogel. Also, at MBA concentrations higher than 0.03 mol/L, the cross linking density of the prepared hydrogels increased, resulting in the formation of shrinked hydrogel network. The shrinkage in turn causes less swelling capacity of hydrogel. As a result, the optimum amount of MBA is 0.03 mol/L in which the synthesized hydrogel had the maximum swelling ratio.

3.3 Effect of AA monomer concentration on swelling behavior

The effect of monomer concentration on equilibrium absorption capacity was investigated by altering the amount of AA monomer. As exhibited in Fig. 5b, by increasing the amount of monomer, the equilibrium absorption capacity increases, so that the highest equilibrium absorption (306 g/g) is obtained at 0.3 mol/L of AA monomer concentration. It should be noted that, AA monomer diffusion in salep polysaccharide structure increments as AA concentration increases, and so are hydrophilicity and equilibrium water absorption of hydrogel. In addition, swelling ratio decreased from 306 to 238 g/g with increasing AA concentration from 0.03 to 0.04 mol/L. This can be attributed to the facts, as follows. At higher AA monomer concentrations than 0.03 mol/L, due to increase in reaction medium viscosity would

end to reduced macro radicals and monomer molecules mobility. Furthermore, probability of homo polymerization is enhanced toward graft polymerization and probability of chain transfer is increased between monomer molecules. As a result, the equilibrium water absorption capacity is decreased.

3.4 Effect of APS initiator concentration on swelling behavior

The effect of APS initiator concentration on equilibrium water absorption capacity is given in Fig. 5c. According to the equilibrium absorption trend in relation with altering the APS concentration, the highest equilibrium absorption capacity (303 g/g) is when the APS concentration is 0.022 mol/L. The increase in equilibrium absorption capacity along with increasing the amount of APS is because of the increase in monomer radical species, macro radical polysaccharides, and monomer grafting on polysaccharide structure probability. It should be mentioned that by over increasing the amount of initiator, the probability of the chain termination between salep macro molecules increases and the salep chains crosslink with each other. Besides, the destructive nature of sulfate anion toward salep radicals in too high concentration of initiator is another reason for lower equilibrium absorption capacity.

3.5 Effect of MMT content on swelling behavior of Hyd/MMT

The effect of MMT content on equilibrium absorption capacity of Hyd/MMT nanocomposite hydrogel is shown in Fig. 5d. The obtained results confirms that water absorption capacity of the Hyd/MMT nanocomposite hydrogel increased from 301 to 328 g/g when MMT content rose from 5 to 20 wt%, respectively. The high electrostatic repulsive forces between negatively charged surface of crystalline structure of MMT and COO⁻ groups of polymeric chains of hydrogel causes an expanded hydrogel network which is responsible for porosity of hydrogel network and enhancement in swelling ratio. However, swelling ratio decreased from 328 to 261 g/g with increasing MMT content from 20 to 30 wt%, respectively. This can be related to the physical cross-linking density increment which is due to enhanced interactions between surface of MMT and polymeric component of the hydrogel. As a result, the void spaces between polymer chains diminish and so is the water absorbency of the nanocomposite [27].

### 3.6 Effect of solution pH on swelling behavior of Hyd/MMT

The equilibrium absorption capacity of synthesized Hyd/MMT nanocomposite was investigated in pH range from 2 to 12 at room temperature. As shown in Fig. 6a, it is clear that with increasing the pH up to 4, the equilibrium absorption capacity increase. This is in relation with protonation of most of the hydrogel carboxylate anions, therefore repulsion forces between carboxylate groups are decreased and causes structure shrinkage. On the other hand, in this range of pH, hydrogen bonds are created between carboxylic groups of hydrogel and hydroxyl groups of MMT which cause more cross-linking in hydrogel nanocomposite network. In basic conditions (pH more than 10), because of the existence of sodium cations of NaOH in solution, COO⁻ groups of hydrogel polymeric chains are protected and so that the repulsion force between chains is decreased, resulting in equilibrium absorption capacity reduction. On the other hand, by increasing the pH, aggregation of carboxylate ions in network structure of nanocomposite hydrogel weakens the hydrogen bands between water molecules and carboxylate groups that forces the water molecules out of the network. Finally, the network is shrinked and equilibrium absorption capacity is decreased. Figure 6b shows a schematic of hydrogel behavior in acidic, neutral and basic environment.

3.7 Effect of saline solution on swelling capacity of Hyd/MMT

The equilibrium swelling capacity of synthesized Hyd/MMT samples were investigated in NaCl, CaCl₂ and FeCl₃ solutions. The effect of NaCl solution concentration on equilibrium swelling capacity is shown in Fig. 7a. The equilibrium swelling capacity is decreased with increasing

Fig. 6 Equilibrium swelling dependency of Hyd/MMT on pH (**a**), and schematic behavior in solution with different pH (**b**)
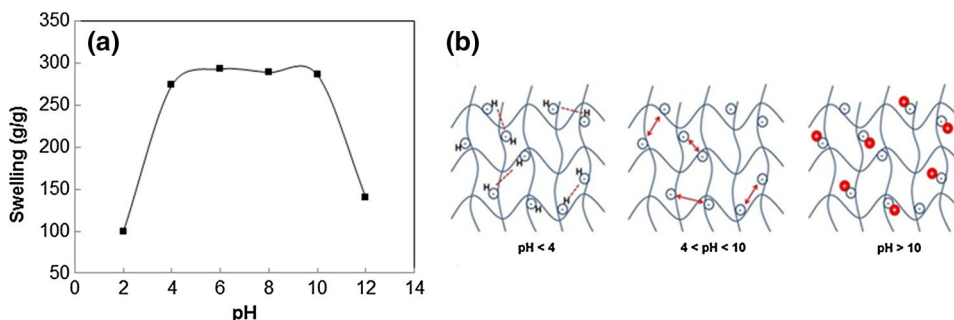
Fig. 7 Equilibrium swelling of Hyd/MMT in various concentration of NaCl solutions (**a**), and in 1 mol/L solutions of NaCl, CaCl₂ and FeCl₃ (**b**)
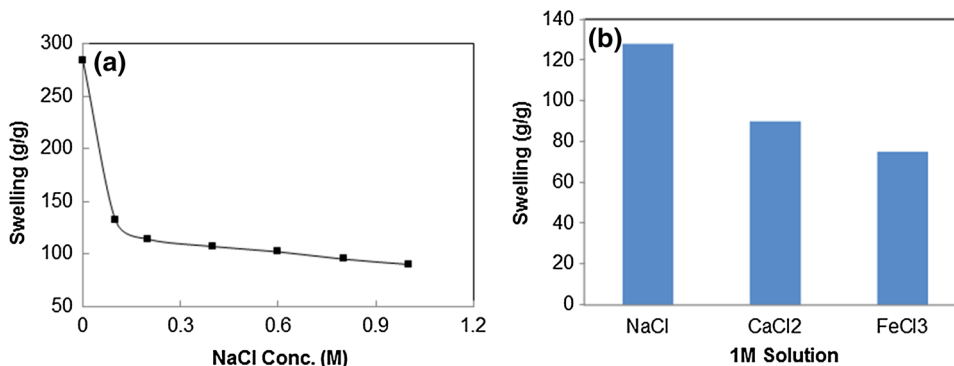
salt concentration. This behavior is related to osmosis pressure and hydrogel network elastisation. The osmosis pressure is obtained from the differential ion concentrations in hydrogel network and outer solution. Counter ions diffusion in hydrogel network causes a decrease in osmosis pressure between hydrogel network and outer solution and so that, the equilibrium swelling of hydrogel is decreased. Also, excess amounts of cations in solution caused the shield effect on carboxylate anions in hydrogel network and reduced repulsion forces between anionic chains. All these made the hydrogel network less expanded. Figure 7b, shows the different salts effect on equilibrium swelling of

nanocomposite hydrogel. As shown, equilibrium swelling capacity in saline solutions is $Na^+>Ca^{2+}>Fe^{3+}$. In multi valence cations such as Ca^{2+} and Fe^{3+}, a complex is created between hydrogel carboxylate groups and these cations, which cause more cross linking in hydrogel. Also, this phenomenon prevents more expansion of hydrogel network and so that, the swelling capacity is decreased [14]. By increasing the cation charge from 2+ to 3+, because of the electrostatic attraction increase, cross linking degree is increased, ending in lower swelling capacity.

### 3.8 Effect of MMT content on swelling kinetic of Hyd/MMT

Water absorption kinetic of hydrogel and nanocomposite hydrogel was studied by Eqs. (2)–(9). Also, the effect of MMT content on water absorption and swelling kinetic of Hyd/MMT nanocomposite samples was studied by investigating the K_s (swelling coefficient), W_∞ (equilibrium amount of absorbed water), k (specific coefficient of hydrogel), n (specific diffusion mechanism exponent), D (diffusion coefficient), and K_w (water absorption rate coefficient) (Fig. 8).

The t/W versus t diagram for Hyd and Hyd/MMT nanocomposite samples with different MMT content are shown in Fig. 9a. Slope and intercept of these diagrams, respectively represent k_s and W_∞. These parameters are given in Table 1. According to data presented in Table, swelling rate coefficient (k_s) is increased by adding MMT. Addition of
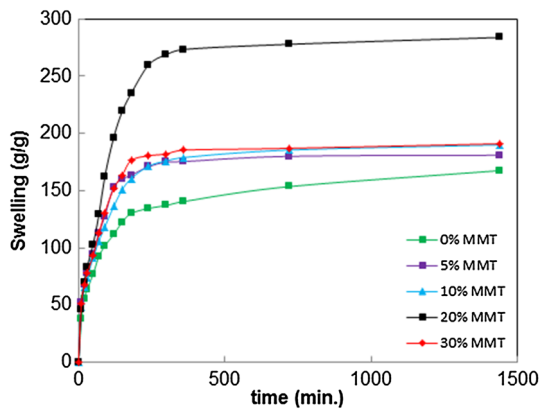
Fig. 8 The kinetic of water absorption for the Hyd and Hyd/MMT with different %MMT

Fig. 9 Swelling kinetic curves of Hyd and Hyd/MMT samples in distilled water
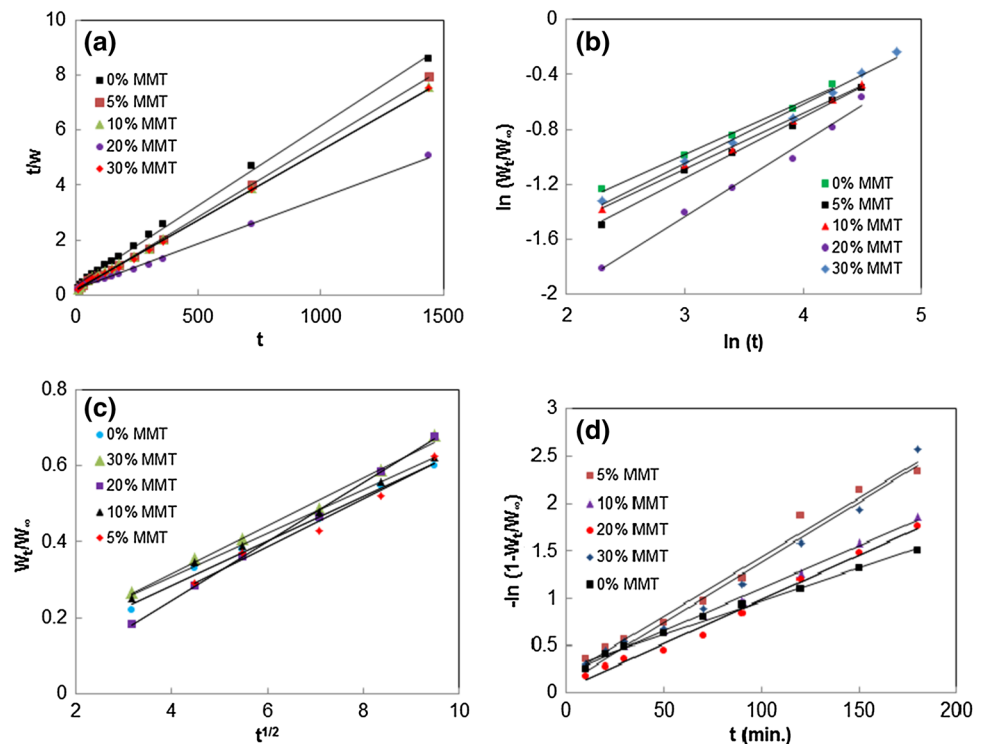
Table 1 Swelling and diffusion parameters of Hyd and Hyd/MMT in distilled water

Equation	Parameter	Hydrogel	MMT5%	MMT10%	MMT20%	MMT30%
$\frac{t}{W} = A + Bt$	k_s	9.59×10^{-5}	1.75×10^{-4}	1.13×10^{-4}	5.23×10^{-4}	1.43×10^{-4}
	W_∞	172.41	185.19	196.08	303.03	196.08
$\frac{W_t}{W_\infty} = kt^n$	k	0.11	0.08	0.10	0.04	0.01
	n	0.3866	0.5434	0.5027	0.5393	0.5295
	D	4.73×10^{-10}	5.40×10^{-10}	5.47×10^{-10}	8.24×10^{-10}	5.53×10^{-10}
$W_t = W_\infty(1 - e^{-k_w t})$	k_w	0.0071	0.0125	0.009	0.0094	0.0128

MMT causes an increase in surface area of hydrogel nanocomposite causing the increase in water molecules diffusion into the hydrogel network and water absorption rate. Theoretical amounts for equilibrium water absorption of Hyd and Hyd/MMT nanocomposite samples are close to experimental amounts.

When a polymeric hydrogel is immersed in a solution, it penetrates into the hydrogel matrix and makes it swollen. Swelling of polymeric hydrogel forces the chains to move and because of this movement, a free space is created between the chains. So to investigate the water diffusion nature, Eq. (2) is used for initial 60% of water absorption. Figure 9b shows the ln (W_t/W_∞) versus ln (t) diagram for Hyd and Hyd/MMT nanocomposite samples with different MMT content. Kinetic parameters such as n and k which are given in Table 1 were obtained from the slope and intercept of curve. As it is seen in Table 1, n value for Hyd is <0.5 but it is more than 0.5 for Hyd/MMT nanocomposite samples. So that the diffusion mechanism for Hyd/MMT nanocomposite is Fickian diffusion but for neat hydrogel it is non-Fickian or anomalous diffusion. It should be concerned that, in non-Fickian diffusion, solvent diffusion and resting rate of polymer are comparable. On the other hand, rest rate of polymer is low because by penetrating the solvent into the hydrogel, chain rearrangement does not happen rapidly.

Figure 9c shows the (W_t/W_∞) versus $t^{1/2}$ diagram for Hyd and Hyd/MMT nanocomposite samples with different MMT contents. From the slope of these lines, diffusion coefficients for hydrogel and nanocomposite hydrogels are obtained and given in Table 1. By adding MMT, diffusion coefficient is increased from 4.73×10^{-10} in neat hydrogel to 8.24×10^{-10} in Hyd/MMT nanocomposite with 20 wt% of MMT content. This indicates that MMT presence in nanocomposite structure facilitates water penetration into hydrogel network.

The $-\ln(1 - W_t/W_\infty)$ versus t diagram for Hyd and Hyd/MMT nanocomposite samples with different MMT contents is shown in Fig. 9d. Water absorption rate coefficient (K_w) is another important diffusion parameter, which is given in Table 1 for different hydrogel samples. Water absorption rate coefficient for Hyd sample is less than its value for Hyd/MMT nanocomposite samples, which is

related to the porous structure of hydrogel nanocomposite. These results are in complete accordance whit SEM images.

In conclusions, a novel porous Hyd/MMT nanocomposite was prepared successfully by graft polymerization of AA on salep in the presence of MMT clay. All of the effective parameters on water uptake and kinetic properties of hydrogel such as monomer, crosslinker, initiator, and clay concentration were optimized. Obtained results from FTIR analysis confirmed that graft polymerization of AA on salep and incorporation of MMT in hydrogel structure were successful. XRD pattern of hydrogel nanocomposite showed that MMT layers were separated and an exfoliated nanocomposite was produced. Furthermore, SEM images of samples revealed that the incorporation of MMT clay in hydrogel structure created a porous morphology. Creating a porous structure increases equilibrium swelling capacity as well as water absorption rate of Hyd/MMT nanocomposite in comparison with neat hydrogel. It is worth to highlight this point that diffusion mechanism for Hyd/MMT nanocomposite hydrogel and neat hydrogel are Fickian (n > 0.5) and non-Fickian (n < 0.5), respectively. Finally, it is concluded that the prepared Hyd/MMT nanocomposite is a promising material as water reservoir for agricultural and horticultural applications.

Compliance with ethical standards

Conflict of interest The authors declare that they have no conflict of interest.

References

1. Y. Dahman, J.E. Puskas, A. Margaritis, Z. Merali, M. Cunningham, Macromolecules **36**(7), 2198 (2003)
2. R.P. Singh, G. Karmakar, S. Rath, N. Karmakar, S. Pandey, T. Tripathy, J. Panda, K. Kanan, S. Jain, N. Lan, Polym. Eng. Sci. **40**(1), 46 (2000)
3. Y. Teramoto, Y. Nishio, Polymer **44**(9), 2701 (2003)

675

4. F.L. Buchholz, A.T. Graham, *Modern superabsorbent polymer technology* (Wiley, New York, 1998), p. 279
5. J. Preston, H. Mark, N. Bikales, C. Overberger, G. Menges, H.F. Mark, in *Encyclopedia of polymer science and engineering*, vol. 11, 2nd edn, ed. by H.F. Mark (Wiley, New York, 1988), p. 381
6. R. Po, J Macromol Sci Part C **34**(4), 607 (1994)
7. A. Schiller, T. Suen, Ind. Eng. Chem. **48**(12), 2132 (1956)
8. S. Yang, Y. Fu, S.H. Jeong, K. Park, J. Pharm. Pharmacol. **56**(4), 429 (2004)
9. S. Kaya, A.R. Tekin, J. Food Eng. **47**(1), 59 (2001)
10. G. Ktistis, P. Georgakopoulos, Pharmazie **46**(1), 55 (1991)
11. R. Farhoosh, A. Riazi, Food Hydrocoll. **21**(4), 660 (2007)
12. A. Pourjavadi, R. Soleyman, G.R. Barajee, Starch-Stärke **60**(9), 467 (2008)
13. G. R. Bardajee, A. Pourjavadi, R. Soleyman, N. Sheikh, Nucl. Instrum. Methods Phys. Res. Sect. B **266**(18), 3932 (2008)
14. A. Pourjavadi, H. Ghasemzadeh, R. Soleyman, J. Appl. Polym. Sci. **105**(5), 2631 (2007)
15. G. B. Marandi, G. R. Mahdavinia, S. Ghafary, J. Polym. Res. **18**(6), 1487 (2011)
16. E. Karadağ, Ö.B. Üzüm, D. Saraydin, Mater. Des. **26**(4), 265 (2005)
17. F. Song, L.-M. Zhang, J.-F. Shi, N.-N. Li, Colloids Surf. B **81**(2), 486 (2010)
18. N. Işıklan, J. Appl. Polym. Sci **105**(2), 718 (2007)
19. A. Pourjavadi, R. Soleyman, G. Rezanejad Bardajee, Iran. J. Chem. Chem. Eng. **29**, 4 (2010)
20. P.L. Ritger, N.A. Peppas, J. Controll Release **5**(1), 37 (1987)
21. H. Kaşgöz, A. Durmus, Polym. Adv. Technol. **19**(7), 838 (2008)
22. T. Singh, R. Singhal, J. Appl. Polym. Sci. **125**(2), 1267 (2012)
23. A. Olad, A. Rashidzadeh, Fibers Polym. **13**(1), 16 (2012)
24. A. Olad, A. Rashidzadeh, M. Amini, Adv. Polym. Tech **32**, 2 (2013)
25. A. Bortolin, F.A. Aouada, L.H. Mattoso, C. Ribeiro, J. Agric. Food. Chem. **61**(31), 7431 (2013)
26. P.J. Flory, *Principles of Polymer Chemistry* (Cornell University Press, Ithaca, 1953)
27. A. Olad, H. Gharekhani, A. Mirmohseni, A. Bybordi, Polym. Bull. **74**, 3353 (2017)